Storing electrons from H2 for transfer to CO2, all at room temperature

COMMUNICATION

Storing electrons from H₂ for transfer to CO₂, all at room temperature†

Daiki Shimauchi, [a,b] Takeshi Yatabe, [a,b,c] Yuka Ikesue, [a,b] Yuu Kajiwara, [a,b] Taro Koide, [a,b] Tatsuya Ando, [a,b,c] Ki-Seok Yoon, [a,b,c] Hidetaka Nakai [d] and Seiji Ogo [a,b,c]*

We present an Ir complex that extracts electrons from H₂ at room temperature and stores them as H₂-derived energy carrier (H₂EC) at room temperature. Further, we demonstrate that this complex reduces CO₂ to a metal-CO₂²⁻ species at room temperature, and present the first electrospray ionisation mass spectrum such a compound.

Much attention is focused on the development of hydrogen energy carriers that meet all the requirements of not requiring much energy for their synthesis, storage and utilisation.[1-4] Metal hydrides,[5] liquid organic hydrides,[6] complex hydrides,[7] ammonia[8] and formic acid[9] have been widely studied as potential hydrogen energy carriers, but no energy carrier has yet met all requirements.

These requirements are directly relevant to our model study of [NiFe]hydrogenase (H₂ase). H₂ase is an enzyme which activates H₂ as an energy source at room temperature,[10,11] and we have made a series of model compounds that mimic such behavior.[12-19] This has led us to produce potential H₂-derived energy carriers (H₂ECs) with all the requirements.

In this paper, we report an H₂EC that is capable of removing electrons from H₂ at room temperature, storing them at room temperature and transferring them to CO₂ at room temperature. Furthermore, we report the first example of direct observation by electrospray ionisation mass spectrometry (ESI-MS) of a metal-CO₂²⁻ species in which CO₂ is reduced by H₂ via reaction with the H₂EC at room temperature. We also present the X-ray structure of a metal alkoxycarbonyl complex isolated from the reaction of the metal-CO₂²⁻ species with an alcohol, also at room temperature. We expect this

complex to point the way to stably storing electrons and energy from H₂.

We begin with the synthesis of the H₂EC (**2**) from Ir^{II} dinuclear complex (**1**) with H₂ (0.1–0.8 MPa) at room temperature. Then, we report the ESI-MS observation of an Ir^{III}-CO₂²⁻ species (**3**), generated by reaction of the H₂EC with CO₂ (0.5 MPa) at room temperature. We then reveal the X-ray structure of an Ir^{III} methoxycarbonyl complex (**4**), prepared by reaction of the Ir-CO₂²⁻ species with methyl alcohol at room temperature. Finally, we discuss the requirements necessary for the H₂EC to both store electrons from H₂ and have them available for CO₂ reduction.

The starting Iridium dinuclear complex [Ir^{II}₂(tpy)₂(CH₃CN)₂(Cl)₂]Cl₂ {[**1**]Cl₂, tpy = 2,2':6',2''-terpyridine} was synthesised by the reaction of [Ir^{I}(COD)(Cl)]₂ (COD = 1,5-cyclooctadiene) with tpy in CH₃CN at room temperature followed by the addition of HCl. Complex **1** was characterised by X-ray analysis (Fig. 1), NMR spectroscopy (Fig. S1), ESI-MS (Fig. S2), X-ray photoelectron spectroscopy (XPS, Figs. S3a and S3c) and elemental analysis. An ORTEP drawing of **1** is shown in Fig. 1. The Ir metal centres both adopt a distorted octahedral geometry and are linked by metal-metal bond. The Ir–Ir distance of **1** {2.7389(7) Å} is comparable to that of previously reported Ir^{II} dimer complexes {2.6584(5)–2.8703(8) Å}.[20]
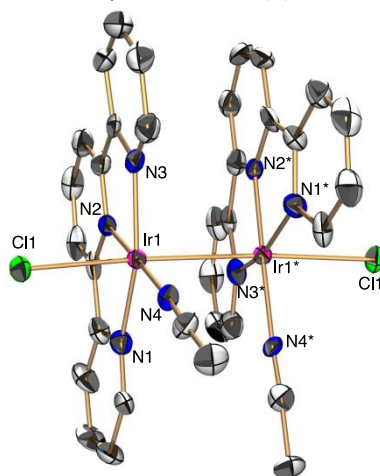
a. *Department of Chemistry and Biochemistry, Graduate School of Engineering, Kyushu University, 744 Moto-oka, Nishi-ku, Fukuoka 819-0395, Japan. E-mail: ogo.seiji.872@m.kyushu-u.ac.jp*

b. *International Institute for Carbon-Neutral Energy Research (WPI Academy I2CNER), Kyushu University, 744 Moto-oka, Nishi-ku, Fukuoka 819-0395, Japan.*

c. *Center for Small Molecule Energy, Kyushu University, 744 Moto-oka, Nishi-ku, Fukuoka 819-0395, Japan.*

d. *Department of Energy and Materials, Faculty of Science and Engineering, Kindai University, 3-4-1 Kowakae, Higashi-Osaka, Osaka 577-8502, Japan.*

Fig. 1 ORTEP drawing of **1** with the ellipsoids at 50% probability. Hydrogen atoms, solvent and counteranion (PF_6) are omitted for clarity. Selected interatomic distances (l/Å): Ir1–Ir1* = 2.7389(7), Ir1–N1 = 2.045(7), Ir1–N2 = 1.953(6), Ir1–N3 = 2.050(6), Ir1–N4 = 2.015(6).

Sharp signals in the diamagnetic region of the ^{1}H NMR spectrum of **1** also suggest the presence of a metal-metal bond between the two Ir^{II} centres (Fig. S1). A positive-ion ESI mass spectrum shows a prominent signal of m/z 461.0 {relative intensity (I) = 100 % in the range of m/z 100–2000}, which has a characteristic isotopic distribution that matched well with the calculated isotopic distribution for half of [**1**–$2CH_3CN$]$^+$ (Fig. S2). An XPS spectrum of **1** shows the peaks at 61.5 and 64.5 eV assigned for Ir $4f_{7/2}$ and Ir $4f_{5/2}$ (Fig. S3a).

Complex **1** reacts with H_2 (0.1–0.8 MPa) in CH_3OH in the presence of CH_3COONa at room temperature to give a low-valent Ir^I complex [Ir^I(tpy)(Cl)] (**2**), H$_2$EC (Eq. 1), which can be stored as a powder at room temperature under N_2 (in a glove box with O_2 below 100 ppm) for at least 3 months.
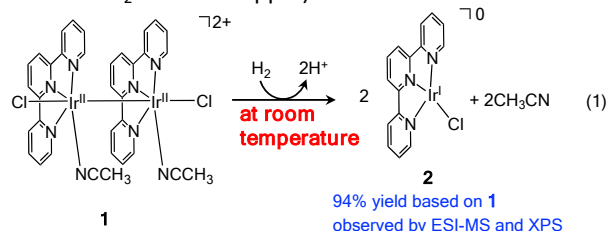

Complex **2** was characterised by UV-vis-NIR absorption spectroscopy (Fig. S4), ESI-MS (Fig. 2), XPS (Figs. S3b and S3d) and elemental analysis. A broad absorption band at 400–1200 nm was observed (Fig. S4), in a similar manner to those also observed in the absorption spectra of previously reported Ir^I polypyridyl complexes.[21] A positive-ion ESI mass spectrum shows a prominent signal at m/z 454.1 (I = 100 % in the range of m/z 100–2000) that corresponds to [**2**–Cl+N_2]$^+$ and has a characteristic isotopic distribution that matched well with the calculated isotopic distribution (Fig. 2). An XPS spectrum of **2** shows the peaks at 61.0 and 63.9 eV, assigned for Ir $4f_{7/2}$ and Ir $4f_{5/2}$ (Fig. S3b). These peaks are lower energy than those of **1** but similar to other Ir^I complexes (Fig. S3).[22] These results indicate complex **2** stores two electrons from H_2 on Ir metal centre as a H$_2$EC at room temperature.
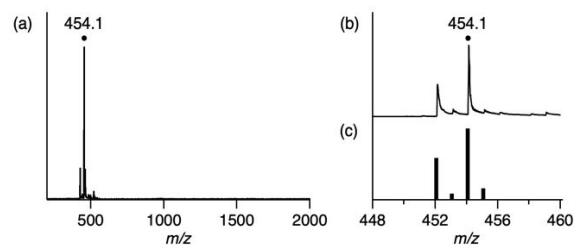
Fig. 2 (a) Positive-ion ESI mass spectrum of **2** in CH_3OH. The signal at m/z 454.1 corresponds to [**2**–Cl+N_2]$^+$. (b) The signal at m/z 454.1 for [**2**–Cl+N_2]$^+$. (c) The calculated isotopic distribution for [**2**–Cl+N_2]$^+$. N_2 is from nebuliser gas of ESI-MS.

Complex **2** reacts with CO_2 (0.5 MPa) in CH_3CN/acetone/CH_2Cl_2 at room temperature to yield

[Ir^{III}(tpy)(COO)(CH_3CN)(Cl)] (a thermodynamically transient species, **3**) (Eq. 2), which was detected by ESI-MS (Figs. 3 and S5). A positive-ion ESI mass spectrum of **3** shows a signal at m/z 547.0 that has a characteristic distribution that matched well with the calculated isotope distribution for [**3**+H]$^+$ (Figs. 3a, 3b and 3c). The reaction of **2** with CO_2 was carried out in acetonitrile-d_3(CD_3CN)/acetone/CH_2Cl_2 gave a D$_3$-labelled **3** [Ir^{III}(tpy)(COO)(CD_3CN)(Cl)] as detected by ESI-MS (Fig. 3d).
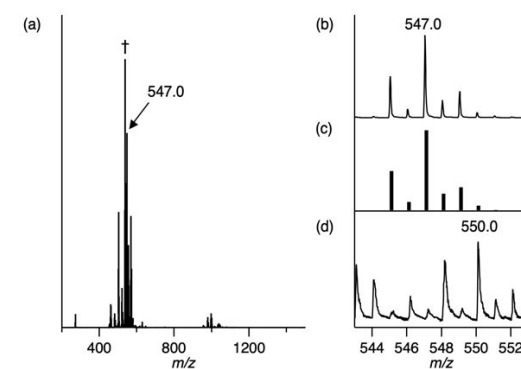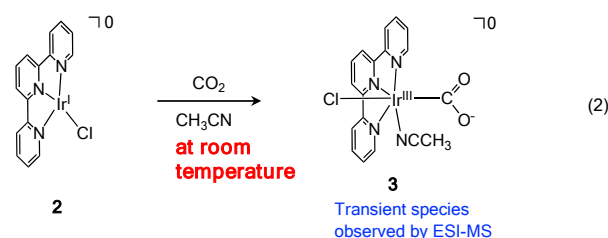
Fig. 3 (a) Positive-ion ESI mass spectrum of a thermodynamically transient **3** in CH_3CN/acetone/CH_2Cl_2. The signal at m/z 547.0 corresponds to [**3**+H]$^+$. †: The signal at m/z 537.0 was assigned as [Ir^{III}(tpy)(Cl)$_2$(CH_3CN)]$^+$, based on the isotope-labelling experiments performed in CD_3CN/acetone/CH_2Cl_2. (b) The signal at m/z 547.0 for [**3**+H]$^+$. (c) The calculated isotopic distribution for [**3**+H]$^+$. (d) Positive-ion ESI mass spectrum of the reaction solution of **2** with CO_2 in CD_3CN/acetone/CH_2Cl_2. The signal at m/z 550.0 corresponds to [D$_3$-labelled **3**+H]$^+$.

This is the first example of the direct observation of metal-CO_2^{2-} species derived from CO_2 and electrons from H_2. The extraction of the electron from H_2 has been performed at room temperature by using hydrogenase model complexes (Table S2).[12-14,16,18,19,23-26] Although the extracted electrons have been used for the reduction of ferrocenium ion, Cu^{II}, O_2 or organic halides at room temperature, there was no example of the reduction of CO_2 at room temperature (Table S2). To date, there have been no low-valent metal complexes synthesised from H_2 that reduce CO_2. In contrast, there are CO_2-complexes synthesized from low-valent metal complexes and CO_2 without H_2 (Table S3).[27–32] For example, Herskovitz et al. reported an Ir-CO_2 complex synthesized from an Ir^I complex.[27,33] Although we tried to perform a ^{13}C-labelling experiment to confirm the source of CO_2 ligand, ^{13}C-labelled complex **3** was not detected due to the inertness of **2** towards $^{13}CO_2$ at only 0.1 MPa. Increasing the pressure of $^{13}CO_2$ gas to suitable levels proved beyond our practical means.

We proceeded to investigate the formation of a metal alkoxycarbonyl complex by the reaction of the in situ-formed **3** and CH_3OH at room temperature. This appeared to be a good target since a similar metal alkoxycarbonyl complex has synthesised from the reaction of Pt-COOH complex with alcohols.[34] The reaction of **2** with CO_2 (0.5 MPa) in CH_3OH/CH_3CN at room temperature gave Ir^{III} methoxycarbonyl complex $[Ir^{III}(tpy)(COOCH_3)(NHCOCH_3)(Cl)]$ (**4**) (Eq. 3). The reaction of **2** with CO_2 and CH_3OH was monitored by UV-vis-NIR absorption spectroscopy (Fig. S6). The absorption band at long wavelength over 400 nm, assigned to **2**, decreased over the course of the reaction.

72% yield based on **2**
observed by ESI-MS and X-ray
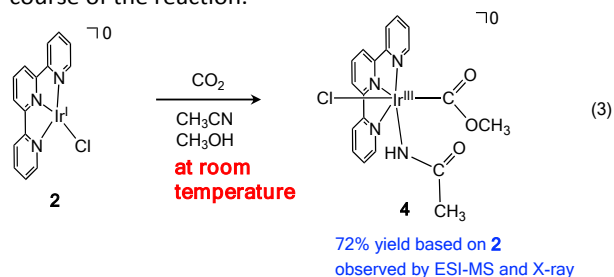
Complex **4** was characterised by NMR (Figs. S7–9) and IR spectroscopy (Fig. S10), X-ray analysis (Fig. 4), ESI-MS (Fig. S11) and elemental analysis. A ^1H NMR spectrum of **4** shows the peaks at 2.40, 3.21 and 7.86–8.81 ppm originating from methoxycarbonyl ligand, acetamido and tpy, respectively (Fig. S7). A ^{13}C NMR spectrum shows a peak at 147.0 ppm derived from C1 atom of methoxycarbonyl ligand, which is similar to those of the reported Ir methoxycarbonyl complexes (Figs. S8 and S9).[35] An IR spectrum of **4** in the solid state shows bands around 1602 cm^{-1}, which are assigned to the C=O stretching vibrations (Fig. S10).[33,35–38]

The structural determination of **4** was conducted by X-ray analysis using a single crystal obtained by diffusion of diethyl ether into the reaction solution. The Ir metal centre adopts a distorted octahedral geometry with tpy, methoxycarbonyl ligand and acetamido (Fig. 4). The bond distances of Ir1–C1 {2.000(4) Å}, C1=O1 {1.209(5) Å} and C1–O2 {1.367(5) Å} and the bond angle of O1=C1–O2 {121.5(4)°} are similar to other alkoxycarbonyl complexes.[33,35,37–38]
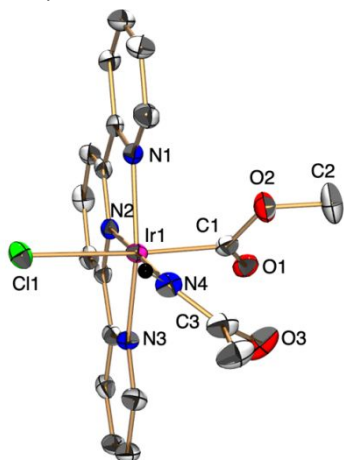

Fig. 4 ORTEP drawing of **4** with the ellipsoids at 50% probability. Hydrogen atoms (except for the NH group) are omitted for clarity. Selected interatomic distances (l/Å): Ir1–C1 = 2.000(4), C1–O1 = 1.209(5), C1–O2 = 1.367(5), Ir1–N1 = 2.053(3), Ir1–N2 = 1.963(3), Ir1–N3 = 2.039(3), Ir1–N4 = 2.044(3), Ir1–Cl1= 2.4817(10).

Isotope-labelling experiments using methanol-d_4 (CD$_3$OD) or CD$_3$CN at room temperature were carried out to investigate the origin of methoxycarbonyl and acetamido ligands (Figs. S11d and S11e). A positive-ion ESI mass spectrum of **4** shows a prominent signal of m/z 543.1 that has isotopic distribution corresponds to the calculated isotopic distribution of [**4**–Cl]$^+$ (Fig. S11a). The reaction of **2** with CO$_2$ was conducted in CH$_3$OH/CD$_3$CN or CD$_3$OD/CH$_3$CN gave a D$_3$-labelled **4** [Ir^{III}(tpy)(COOCH$_3$)(NHCOCD$_3$)(Cl)] (Fig. S11d) or a D$_4$-labelled **4** [Ir^{III}(tpy)(COOCD$_3$)(NDCOCH$_3$)(Cl)] (Fig. S11e), respectively, as confirmed by ESI-MS. To establish the origin of the oxygen atom of acetamido ligand of **4**, an isotope-labelling experiment using H$_2$^{18}O was also conducted. A positive-ion ESI mass spectrum of the reaction of **2** with CO$_2$ in CH$_3$OH/CH$_3$CN in the presence of H$_2$^{18}O shows a prominent signal at m/z 543.1 which has a characteristic isotopic distribution that matches well with the calculated isotopic distribution for [**4**–Cl]$^+$ (Fig. S11f). This means the acetamido ligand is not formed by the hydration of acetonitrile. These isotope-labelling experiments indicate that the coordinated methoxycarbonyl ligands of complex **4** are derived from CO$_2$ and CH$_3$OH, and the acetamido ligands are derived from CH$_3$CN, CH$_3$OH, and CO$_2$ (Fig. S12).

We have elucidated the following design requirements for: 1) synthesising the H$_2$EC, and 2) using it in the reduction of CO$_2$. In the first step, an electron-withdrawing ligand is required to stabilise the low-valent, electron-carrying H$_2$EC. This step requires acetate ions as a Lewis base that abstracts the protons from H$_2$. In the next step, however, an electron-donating ligand is required to stabilise the resulting metal-CO$_2$$^{2-}$ species. Meanwhile, each step requires the H$_2$EC to have a reaction site to activate H$_2$ or CO$_2$. Thus, H$_2$ oxidation (synthesis of the H$_2$EC) and CO$_2$ reduction (utilisation of the H$_2$EC) require ligands with opposite electronic properties. In order to perform these antagonistic processes using a single molecule, some sacrifice in ligand design for either H$_2$ oxidation or CO$_2$ reduction is required. After trial and error with this strategy, we chose tpy, a weakly electron-withdrawing ligand. As a result, we succeeded in accelerating the H$_2$ oxidation to synthesise the H$_2$EC at room temperature and slowing down the CO$_2$ reduction to observe the metal-CO$_2$$^{2-}$ species. This balance results in a H$_2$EC that can perform both functions at room temperature.

Based on the above results, we propose the following reaction mechanism (Fig. 5). The dinuclear Ir^{II} complex (**1**) extracts electrons from one equivalent of H$_2$ to form two equivalents of Ir^I complex (**2**, H$_2$EC) at room temperature, which is stable for at least three months at room temperature under N$_2$ atmosphere. This H$_2$EC is able to use the electrons from H$_2$ to reduce CO$_2$ to CO$_2$$^{2-}$ as part of complex **3** at room temperature. The CO$_2$$^{2-}$ moiety of **3** then reacts with CH$_3$OH to form the methoxycarbonyl complex **4** at room temperature. All three reactions are performed at room temperature.
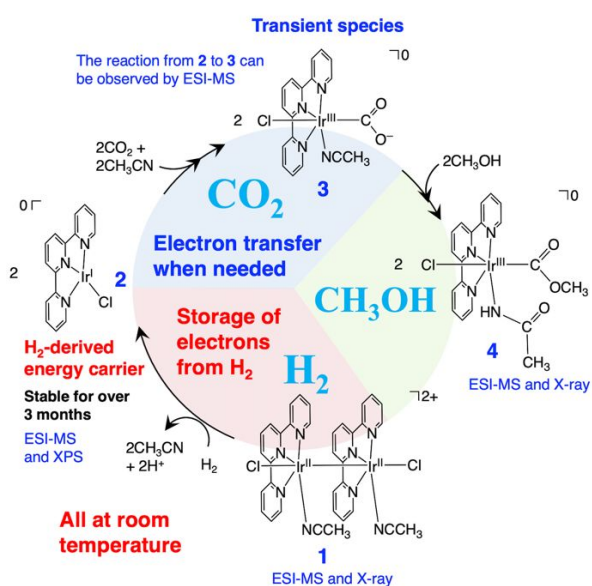
Fig. 5 An Ir^{II} dinuclear complex (**1**) reacts with H$_2$ (0.1–0.8 MPa) to give a low-valent Ir^I complex (**2**, H$_2$EC) at room temperature. The H$_2$EC reacts with CO$_2$ (0.5 MPa) to give an Ir^{III}-CO$_2$$^{2-}$ species (**3**) at room temperature. The Ir^{III}-CO$_2$$^{2-}$ species reacts with CH$_3$OH to give an Ir^{III} methoxycarbonyl complex (**4**) at room temperature.

In conclusion, this study points to a number of specific advantages of an H$_2$EC, which has so much promise. First, this H$_2$EC is produced directly from H$_2$ at room temperature. Second, this H$_2$EC stores electrons from H$_2$ at room temperature. Finally, this H$_2$EC uses H$_2$ to directly reduce CO$_2$ at room temperature to a potential chemical feedstock. As such, we intend to use the lessons learned in this study to drive forward this exciting area of chemistry, filled as it is with so much promise.

Conflicts of interest

There are no conflicts to declare.

References

1 A. Kovač, M. Paranos and D. Marciuš, *Int. J. Hydrogen Energy*, 2021, **46**, 10016–10035.
2 M. D. Allendorf, V. Stavila, J. L. Sinder, M. Witman, M. E. Bowden, K. Brooks, B. L. Tran and T. Autrey, *Nat. Chem.*, 2022, **14**, 1214–1223.
3 M. R. Usman, *Renew. Sustain. Energy Rev.*, 2022, **167**, 112743.
4 J. Yang, A. Sudik, C. Wolverton and D. J. Siegel, *Chem. Soc. Rev.*, 2010, **39**, 656–675.
5 A. Schneemann, J. L. White, S. Y. Kang, S. Jeong, L. F. Wan, E. S. Cho, T. W. Heo, D. Prendergast, J. J. Urban, B. C. Wood, M. D. Allendorf and V. Stavila, *Chem. Rev.*, 2018, **118**, 10775–10839.
6 P. Preuster, C. Papp and P. Wasserscheid, *Acc. Chem. Res.*, 2017, **50**, 74–85.
7 T. He, H. Cao and P. Chen, *Adv. Mater.*, 2019, **31**, 1902757.
8 K. E. Lamb, M. D. Dolan and D. F. Kennedy, *Int. J. Hydrogen Energy*, 2019, **44**, 3580–3593.
9 N. Onishi, G. Laurenczy, M. Beller and Y. Himeda, *Coord. Chem. Rev.*, 2018, **373**, 317–332.
10 W. Lubitz, H. Ogata, O. Rüdiger and E. Reijerse, *Chem. Rev.*, 2014, **114**, 4081–4148.
11 H. Ogata, K. Nishikawa and W. Lubitz, *Nature,* 2015, **520**, 571–574.
12 T. Matsumoto, B. Kure and S. Ogo, *Chem. Lett.*, 2008, **37**, 970–971.
13 D. Inoki, T. Matsumoto, H. Hayashi, K. Takashita, H. Nakai and S. Ogo, *Dalton Trans.*, 2012, **41**, 4328–4334.
14 D. Inoki, T. Matsumoto, H. Nakai and S. Ogo, *Eur. J. Inorg. Chem.*, 2013, 3978–3986.
15 S. Ogo, L. T. T. Minh, T. Kikunaga, T. Ando, T. Matsumoto, T. Yatabe and K. Kato, *Organometallics*, 2020, **39**, 3731–3741.
16 T. Yatabe, K. Kamitakahara, K. Higashijima, T. Ando, T. Matsumoto, K.-S. Yoon, T. Enomoto and S. Ogo, *Chem. Commun.*, 2021, **57**, 4772–4774.
17 T. Yatabe, S. Futakuchi, K. Miyazawa, D. Shimauchi, Y. Takahashi, K.-S. Yoon, H. Nakai and S. Ogo, *RSC Adv.*, 2021, **11**, 39450–39454.
18 T. Yatabe, T. Tome, Y. Takahashi, T. Matsumoto, K.-S. Yoon, H. Nakai and S. Ogo, *Chem.–Eur. J.*, 2021, **27**, 17326–17330.
19 S. Ogo, T. Yatabe, T. Tome, R. Takenaka Y. Shiota and K. Kato, *J. Am. Chem. Soc.*, 2023, **145**, 4384−4388.
20 J. F. Berry, *Metal-Metal Bonded Compounds of the Group IX Elements*. In *Reference Module in Chemistry, Molecular Sciences and Chemical Engineering*, Elsevier, 2021, pp 4–42.
21 K. Garg, Y. Matsubara, M. Z. Ertem, A. Lewandowska-Andralojc, S. Sato, D. J. Szalda, J. T. Muckerman and E. Fujita, *Angew. Chem. Int. Ed.*, 2015, **54**, 14128– 14132.
22 M. Y. Smirnov, A. V. Kalinkin, L. M. Kovtunova and V. I. Bukhtiyarov, *Surf. Interfaces*, 2021, **25**, 101176.
23 J. Y. Yang, S. E. Smith, T. Liu, W. G. Dougherty, W. A. Hoffert, W. S. Kassel, M. R. DuBois, D. L. DuBois and R. M. Bullock, *J. Am. Chem. Soc.*, 2013, **135**, 9700–9712.
24 H. Nakai, K. Jeong, T. Matsumoto and S. Ogo, *Organometallics*, 2014, **33**, 4349–4352.
25 Y. Zhang, T. J. Woods and T. B. Rauchfuss, *J. Am. Chem. Soc.*, 2021, **143**, 10065–10069.
26 C. Takahashi, T. Yatabe, H. Nakai and S. Ogo, *Chem.–Eur. J.*, 2023, DOI: 10.1002/chem.202302297
27 T. Herskovitz, *J. Am. Chem. Soc.*, 1977, **99**, 2391–2392.
28 G. S. Bristow, P. B. Hitchcock and M. F. Lappert, *J. Chem. Soc., Chem. Commun.*, 1981, 1145–1146.
29 J. C. Calabrese, T. Herskovitz and J. B. Kinney, *J. Am. Chem. Soc.*, 1983, **105**, 5914–5915.
30 H. G. Alt, K.–H. Schwind and M. D. Rausch, *J. Organomet. Chem.,* 1987, **321**, C9–C12.
31 D. W. Lee, C. M. Jensen and D. Morales-Morales, *Organometallics,* 2003, **22**, 4774–4749.
32 I. Castro-Rodriguez, H. Nakai, L. N. Zakharov, A. L. Rheingold and K. Meyer, *Science*, 2004, **305**, 1757–1759.
33 R. L. Harlow, J. B. Kinney, T. Herskovitz, *J. Chem. Soc., Chem. Commun.*, 1980, 813–814.
34 M. A. Bennett, G. B. Robertson, A. Rokicki and W. A. Wickramasinghe, *J. Am. Chem. Soc.*, 1988, **110**, 7098–7105.
35 L. Dahlenburg and K. Herbst, *J. Chem. Soc., Dalton Trans.,* 1999, 3935–3939.
36 M. A. Esteruelas, L. A. Oro, R. M. Claramunt, C. López, J. L. Lavandera and J. Elguero, *J. Organomet. Chem.*, 1989, **366**, 245–255.
37 P. K. Chan and W. K. Leong, *Organometallics*, 2008, **27**, 1247–1253.
38 W. I. Dzik, J. M. M. Smits, J. N. H. Reek and B. Bruin, *Organometallics*, 2009, **28**, 1631–1643.